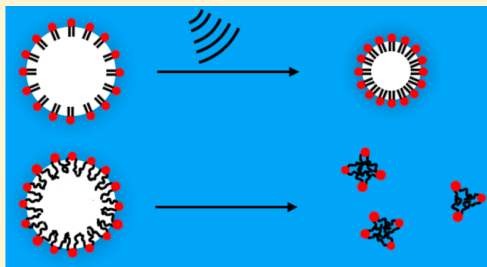


Temperature-Dependent Biphasic Shrinkage of Lipid-Coated Bubbles in Ultrasound

Debra J. Cox and James L. Thomas*

Department of Physics and Astronomy, University of New Mexico, Albuquerque, New Mexico 87131, United States

ABSTRACT: Lipid-coated microbubbles and emulsions are of interest as possible ultrasound-mediated drug delivery vehicles and for their interesting behaviors and fundamental properties. We and others have noted that bubbles coated with the long chain saturated phospholipid distearoylphosphatidylcholine (DSPC) rapidly shrink to a quasistable size when repeatedly insonated with short ultrasound pulses; such stability may adversely affect the bubble's subsequent ability to deliver its pharmacological cargo. Bubbles coated with the unsaturated lipid dioleoylphosphatidylcholine (DOPC) did not show stability but did undergo an abrupt change from rapid initial shrinkage to a slow persistent shrinkage, leading ultimately to dissolution or dispersion. As DOPC and DSPC differ not only in chain saturation but also phase behavior, we performed additional studies using dimyristoyl PC (DMPC) as a coat lipid and controlled the solution temperature to study bubble behavior on exposure to repeated ultrasound pulses for the same coat, in both fluid and gel phases. We find, first, that essentially all bubbles show an initially rapid shrinkage, in which gas loss exceeds the limit imposed by gas diffusion into the surrounding medium; this rapid shrinkage may be evidence of nanoscopic bubble fragmentation. Second, upon reaching a fraction of their initial size, bubbles begin a slower shrinkage with a shrinkage rate that depends on the resting phase state of the coat lipid: fluid DMPC monolayers give a more rapid shrinkage than gel phase. DOPC-coated bubbles showed no temperature-dependent responses in the same temperature range. The results are especially interesting in that bubble compression during the pulse is likely to adiabatically heat the bubble and fluidize the coat, regardless of its initial phase state; thus, some structural feature of the resting coat, such as defect lines in the gel phase, may be important in the subsequent response to the $\sim 3 \mu\text{s}$ ultrasound pulse.



1. INTRODUCTION

There is growing interest in the application of lipid-coated bubbles or emulsions to ultrasound-targeted drug delivery.^{1,2} An attractive feature of these vehicles is that they can be disrupted or dispersed by ultrasound levels that are not damaging to healthy tissues. Disruption may enhance the local efficacy of pharmacologically active compounds via a number of proposed mechanisms including repartitioning,³ chemical cleavage,⁴ or enhanced fragment uptake by cells.⁵ Because of the role of bubble or droplet disruption in delivery, it is important to elucidate the role of the lipid coat in determining the fate of bubbles or droplets exposed to ultrasound.

For lipid-coated gas bubbles, the selection of the appropriate lipid coat is in part determined by the desirability of stabilizing the (resting) bubbles, so as to provide a relatively large time window in which they can be used effectively after their preparation. Micron-sized uncoated gas (nitrogen or oxygen) bubbles rapidly dissolve in the blood, in a few seconds.⁵ For targeted delivery applications, it is essential to have stability that exceeds the circulation time, about 1 min, and desirable to have bubbles remain stable for perhaps an order of magnitude longer, to minimize untargeted release. Stabilization is aided by using a very poorly soluble gas, such as perfluorobutane (PFB), but even with PFB, Laplace pressure arising from bubble surface tension tends to drive the gas into the surrounding solution.⁶ For the best stability in ultrasound imaging, long

chain saturated lipids (e.g., distearoylphosphatidylcholine) are often used; long chain saturated lipids are an important component of Definity, a commercial bubble formulation for ultrasound imaging. We^{7,8} and others^{9,10} have observed that DSPC-coated PFB bubbles typically shrink rapidly when exposed to repeated pulses of megahertz ultrasound but that these bubbles usually reach a stable size and are subsequently unresponsive, at least to the extent that no further size changes are microscopically observable with the same pulse amplitude and duration. Such stability may well be undesirable from a delivery perspective, as the remaining bubble may sequester a large fraction of the drug to be delivered. It is generally possible to destabilize the bubbles by using stronger insonation,⁹ but such changes in the insonation protocol may be undesirable and add uncertainty as to the extent of release.

In an earlier study,⁷ we observed that bubbles coated primarily with the long chain unsaturated phospholipid dioleoylphosphatidylcholine (DOPC) also showed a rapid initial shrinkage but that, rather than reach a fully stable size, they show a very slow shrinkage and ultimately do vanish through complete dissolution or nanoscopic (i.e., microscopically invisible) fragmentation. DOPC has both chemical (bond

Received: February 8, 2013

Revised: March 14, 2013

Published: March 14, 2013

unsaturation) and physical (monolayer phase) differences, compared with DSPC; in principle, either or both differences could be responsible for different responses to insonation, especially given that ultrasound can often enhance chemical reactivity via the generation of radicals.^{11,12}

To gain further insight into the role of the lipid coat in ultrasound responsiveness, we undertook a study of the behavior of dimyristoylphosphatidylcholine (DMPC)-coated PFB bubbles, with the sample temperature varied between 4 and 26 °C. The rationale is that if lipid phase (gel vs fluid) can play an important role in bubble stability, then DMPC-coated bubbles should show a temperature-dependent response to insonation, with more stable bubbles obtained at lower temperatures. DMPC was chosen because DOPC lipid bilayers and monolayers solidify below 0 °C, and thus solid or gel phase DOPC coats are unrealizable in aqueous buffers.

2. MATERIALS AND METHODS

2.1. Materials. Perfluorobutane (PFB) was purchased from SynQuest (Alachua, FL). Phospholipids 1,2-dimyristoyl-*sn*-glycero-3-phosphocholine (DMPC) and 1,2-dioleoyl-*sn*-glycero-3-phosphocholine (DOPC) were purchased from Avanti Polar Lipids (Alabaster, AL). Phosphate buffered saline (PBS) was prepared with 100 mM NaCl and 40 mM Na₂HPO₄ in nanopure water (D13321, Barnstead, Dubuque, IA) and pH adjusted to 7.4 using HCl (measured with a UB-10 Denver Instrument pH meter (Arvada, CO)).

2.2. Bubble Preparation. Lipid-coated PFB bubbles were prepared by entrainment of gas bubbles in a lipid suspension via probe sonication at the gas/fluid interface, as described elsewhere.^{7,13,14} Lipid coats consisted of 100% DMPC or 100% DOPC. (As the bubbles were used shortly after preparation, stabilizing PEG-lipids were not needed or included. Bubbles without PEG will more easily coalesce, but these bubbles were diluted such that there was only one or two in each field of view (140 μm across), so they were unlikely to encounter another bubble.) The lipid suspension was prepared as follows: the appropriate amount of lipid (dissolved in chloroform) was measured out into a glass vial, and chloroform was removed by nitrogen evaporation followed by vacuum desiccation for 1 h. The lipid, which now appears as a thin, opaque film in the vial, was suspended at 5 g/L in PBS by vortex mixing (VM-3000, VWR) at room temperature until the lipid film was removed from the vial wall. The lipid suspension was then probe sonicated (VC 130PB, Sonics & Materials, Newton, CT), with the sonicator tip near the bottom of the vial, at 30/100 power (~1 W) for 15 min.

To make lipid-coated bubbles, a 0.25 mL aliquot of the lipid suspension was put in a 2 mL glass vial capped with a septum with a hole for the probe sonicator tip to go through. The sonicator tip was positioned at the gas/fluid interface, the vial headspace was flushed with PFB, and probe sonicator was turned on at maximum power (~10 W) for 10 s. The vial was immediately cooled in an ice bath after sonication. After about 15 s on ice, bubbles were diluted 1:100 in PBS and put in the sample chamber (a specially designed 3 mL rectangular cuvette made out of 5 mil PVC, chosen for its high optical and acoustic (~99%) transmissivity).

The PBS was either air saturated (where no particular effort was made to change the dissolved gas) or PFB saturated. To saturate PBS with PFB, 4 mL of PBS was put in a glass vial capped with a septum, PFB was bubbled through the PBS for 30 s, and the vial was left at room temperature for at least 24 h. To get the PFB saturated PBS into the sample chamber without exposing it to air, the cuvette cap on the sample chamber was replaced with a cuvette cap with a hole cut in it and a septum glued to it, and the sample chamber was filled with PFB gas. PFB saturated PBS was retrieved from the vial with a syringe and injected it into the sample chamber, and then bubbles were added (also by injection with a syringe).

2.3. Methods. The sample chamber was positioned in a water bath at the focus of an ultrasound transducer (H-101, Sonic Concepts, Bothell, WA), and the bubbles were insonated with short pulses of

ultrasound and imaged after each pulse (Figure 1A). Ultrasound pulses were generated as described previously.⁷ 1.1 MHz ultrasound was

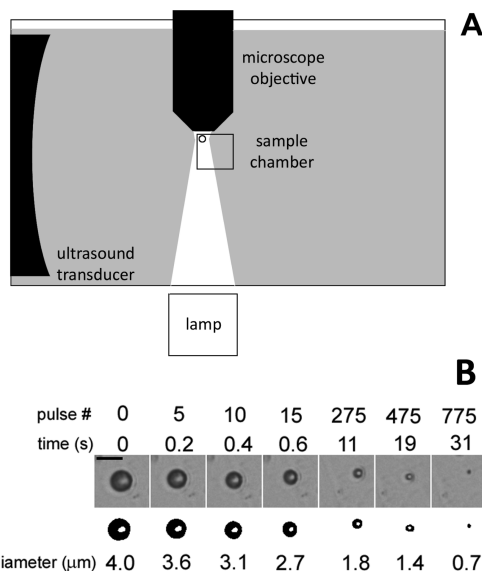


Figure 1. (A) Experimental setup. The sample chamber containing the bubbles is placed in a water tank at the focus of an ultrasound transducer and a water-immersion microscope objective. Bubbles are illuminated from below to form bright-field images. (B) Images of a typical DMPC bubble shrinking in pulsed ultrasound. The scale bar is 5 μm. The number of pulses and the time since the onset of insonation are indicated. The diameter vs time for this bubble is plotted in Figure 2. Bubble diameter was measured by thresholding the images in ImageJ (thresholded images are shown below the raw images), finding the area, and converting that to a diameter (assuming the bubble is circular).

chosen because it provides a more biomedically relevant system than lower frequencies. The sound is focusable to mm dimensions and to high intensity. Three types of pulses with various amplitudes and lengths were used: 3 cycle 200 kPa amplitude, 7 cycle 200 kPa amplitude, and 3 cycle 300 kPa amplitude. All pulses had a frequency of 1.1 MHz and a pulse repetition rate of 25 Hz. When collecting data, we rotated through the three ultrasound pulse types so that each batch of bubbles would be treated in the same way. Bubbles 1–10 μm in diameter were exposed to pulsed ultrasound; bubbles outside this range may be highly nonresonant at 1.1 MHz (5.3 μm is the resonant size).⁷

Bright-field images were taken using a CCD camera (DFK 31BU03, The Imaging Source, Charlotte, NC) and a water immersion microscope objective (LUMPLFLN 40XW NA 0.8, Olympus, Tokyo, Japan), giving a measured resolution of 0.6 μm. The objective was focused on bubbles resting buoyantly against the top surface of the sample chamber and near the edge closest to the ultrasound transducer to minimize effects of attenuation and scattering by other bubbles in the path of the ultrasound pulse. During insonation, images were first collected after each pulse (25 Hz); after shrinkage slowed, images were collected every second or half second. The resulting series of images was analyzed using NIH ImageJ. ImageJ automatically thresholds the images, and the area of the bubble in the thresholded image was measured and converted to an effective radius (Figure 1B).

The ambient temperature was varied by putting ice in the water bath surrounding the sample cuvette. The water bath was initially cooled to 4 °C with ice and was allowed to warm gradually to room temperature (during 1 h). A number of experiments were conducted during this time, by moving the sample to obtain uninsonated bubbles for each new experiment; the temperature was noted for each

experiment. During insonation there was no ice in the water bath, as this might produce unusual patterns of scattered sound.

3. RESULTS AND DISCUSSION

Figure 2 shows typical trajectories of bubble diameter vs time for DMPC- and DOPC-coated bubbles. In these measure-

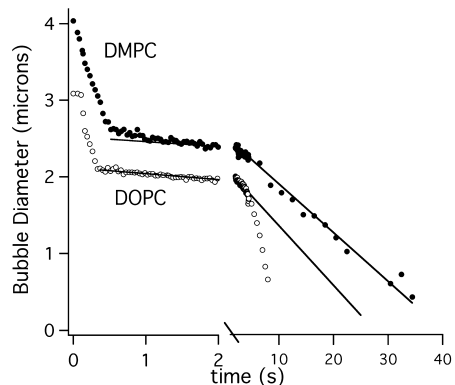


Figure 2. Typical diameter vs time for DMPC and DOPC bubbles exposed to 200 kPa 3 cycle ultrasound pulses. The trajectories show biphasic shrinkage: rapid initial shrinkage, followed by a slow, approximately linear shrinkage. The lines show a linear fit to the first few seconds of the slow shrinkage; the accelerating terminal shrinkage of the DOPC-coated bubble is apparent.

ments, bubbles that rested buoyantly against the top surface of the sample cuvette were exposed to brief ($\sim 3 \mu\text{s}$, 3 cycle) pulses of 1.1 MHz ultrasound, at 200 kPa amplitude. The bubbles initially showed a rapid decrease in size to 1–4 μm in diameter, followed by much slower, approximately linear shrinkage. (Lines on the figure show a linear fit to the first few seconds of slow shrinkage.) Both DMPC-coated and DOPC-coated bubbles eventually vanished. The DOPC-coated bubble shown had an accelerating shrinkage just before complete dissolution, a behavior that was frequently observed with DOPC (28/33) but less frequently with DMPC (30/78).

As we reported previously,⁷ similar biphasic shrinkage was also observed with the long (saturated) chain coat lipid DSPC. With DSPC, the slow shrinkage rate was often zero or near zero, and most bubbles never disappeared from view even after several hundred pulses.

Not all bubbles behaved in the same way; occasionally bubbles would fragment into a small number of microscopically visible parts; this occurred more frequently for DOPC coats than for DMPC coats (Figure 3). In rare instances, bubbles were observed to undergo an approximately linear steady shrinkage. Temperature generally had little effect on the fate of the bubbles (i.e., the fraction of bubbles that showed fragmentation, monophasic steady shrinkage, or biphasic shrinkage), though there was some evidence of slightly increased fragmentation of DMPC bubbles at higher temperatures, with short, more intense pulses (3-cycle, 300 kPa; $p < 0.006$). Other pulse durations, amplitudes, and coats (i.e., DOPC) gave no significant correlations of bubble fate with temperature.

Several features of the bubble behavior are noteworthy. Bubble shrinkage must necessarily involve the loss of the entrapped PFB gas. It has been suggested that the loss of gas into aqueous solution during the 3 μs pulse is negligible, as it is constrained by diffusion.¹⁵ Thus, loss of gas has generally been

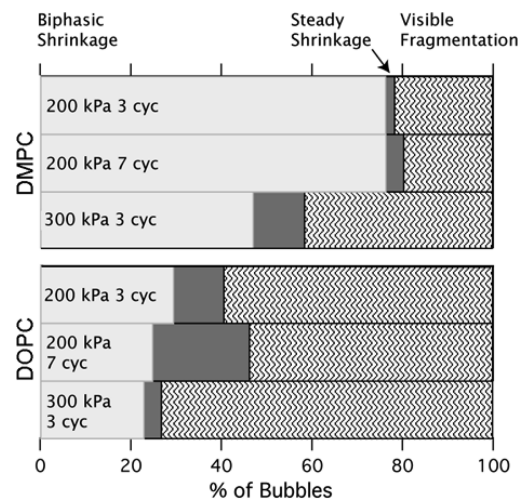


Figure 3. Fraction of bubbles showing various modes of dissolution, for different coat lipids (DMPC, top, and DOPC, bottom) and different pulse durations and amplitudes. Most DMPC-coated bubbles exhibited biphasic shrinkage (Figure 2), some fragmented into a small number of microscopically visible parts, a few underwent approximately linear “steady shrinkage” (monophasic). There was some evidence of increased fragmentation for DMPC bubbles exposed to 200 kPa 3 cycle pulses ($p < 0.006$); otherwise, temperature had no effect on the qualitative manner of bubble dissolution.

presumed to occur via diffusion into the aqueous buffer in between the brief insonation pulses. (The pulses would still enhance shrinkage via coat shedding, resulting in increased internal pressure.) However, the initial rapid phase of bubble shrinkage is actually faster than can be accomplished via diffusion alone (Figure 4). The diffusion-limited shrinkage of a bubble may be computed from the Epstein–Plesset equation¹⁶

$$\frac{dR}{dt} = -\frac{Dk_H BT}{R} \frac{1-f + \frac{2M_w\sigma}{\rho_B T R}}{1 + \frac{4M_w\sigma}{3\rho_B T R}} \quad (1)$$

using parameter values that maximize shrinkage rate: zero dissolved PFB (at infinity in the bulk solution) and a bubble surface tension equal to that of bare water, 72 dyn/cm. The use of the steady-state EP equation is justified by the fact that the bubbles are resting in buffer for several minutes prior to insonation, allowing for local equilibration. During the rapid initial phase, we observed here that both DMPC and DOPC bubbles shrink faster than can be accounted for by diffusion of gas into the surrounding medium. We have also observed rapid shrinkage with DOPC and DSPC-coated PFB bubbles, as reported previously.⁸

Diffusional limitations on bubble shrinkage can also be measured by observing the shrinkage of uncoated bubbles, in the absence of insonation. As reported previously,⁸ these bubbles shrink much more slowly than insonated bubbles, in spite of their high Laplace pressures, and fall within the EP limit. Additional and compelling evidence of rapid loss of bubble volume was recently obtained by Thomas et al.,¹⁷ who found significant shrinkage of Definity microbubbles during, but not between, 1.6 MHz ultrasound pulses, using a high-speed (13 Mfps) video camera.

Thus, both direct and indirect observations suggest that the initial, rapid shrinkage of these bubbles must be accompanied

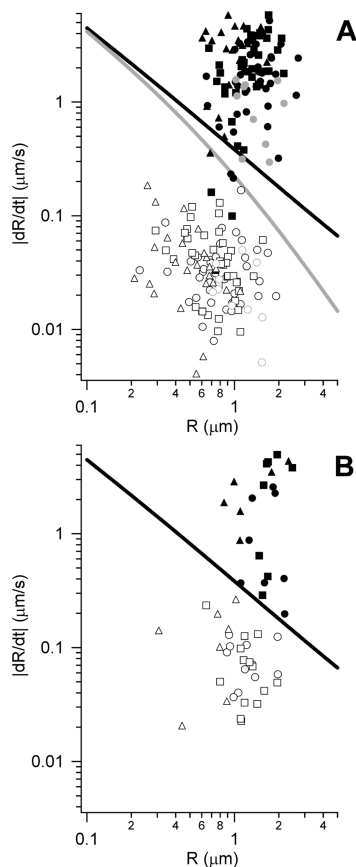


Figure 4. Rate of bubble shrinkage vs radius for DMPC (A) and DOPC (B) bubbles. Filled symbols are the initial rapid shrinkage rate; open symbols are the slower shrinkage rate. Circles are bubbles exposed to 200 kPa 3 cycle pulses, squares are 200 kPa 7 cycle pulses, and triangles are 300 kPa 3 cycle pulses. Black are bubbles in air-saturated buffer, and gray are bubbles in PFB-saturated buffer. The lines show the theoretically maximal (diffusion limited) rates of shrinkage for a completely uncoated, quiescent perfluorobutane bubble (eq 1), in air-saturated buffer ($f = 0$) (black line), or PFB-saturated buffer ($f = 1$) (gray line), calculated for $T = 25$ °C. The rapid shrinkage is faster than the diffusion limit for gas efflux, while the slow shrinkage is not.

by loss of gas by a mechanism other than dissolution into the surrounding medium. We have suggested that these bubbles are fragmenting, with (gas-entrapping) fragments smaller than the optical resolution limit being shed from the bubble surface.⁸

3.1. Transition Diameter and Bubble Lifetime. Figure 5A shows the bubble diameter at which ultrasound-induced shrinkage changed from the rapid phase to the slow phase, plotted against the initial (preinsolation) bubble diameter. There is a strong correlation: shrinkage slows when the bubble diameter is $\sim 60\%$ of the initial diameter or when the surface area is about a third of the initial area. This “memory” of initial bubble size could arise from initial shedding of uncoated bubble fragments (and dissolution of gas into the medium), leaving the coat molecules in place. (Indeed, it is difficult to imagine a mechanism for memory in which coat molecules are not retained.) This suggests that the density of the coat is an important parameter controlling the rate of bubble shrinkage and that whatever mechanism is responsible for rapid initial

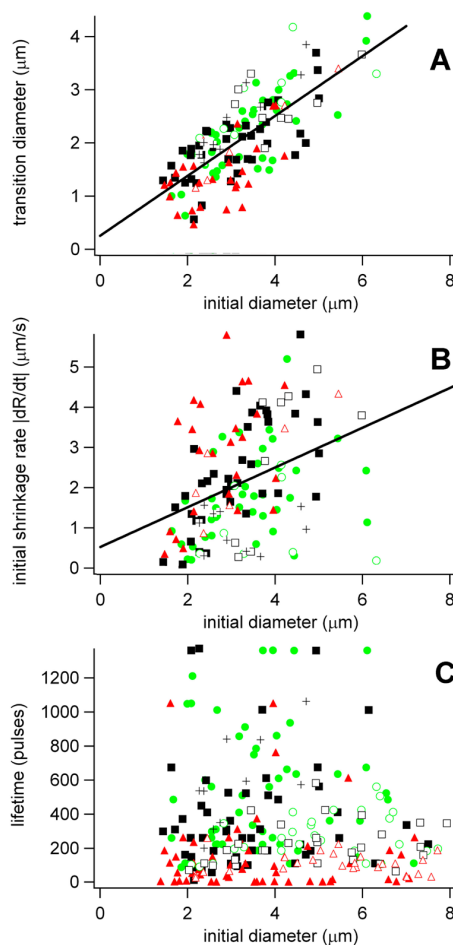


Figure 5. (A) Transition diameter vs initial diameter. The transition diameter is the bubble diameter at which ultrasound-induced shrinkage changed from the rapid phase to the slow phase, and it is correlated with the initial diameter for bubbles coated with both DMPC ($r = 0.7006$, $p = 1.9 \times 10^{-15}$) and DOPC ($r = 0.8078$, $p = 1.05 \times 10^{-6}$). (B) Initial shrinkage rate vs initial diameter. The initial shrinkage rate is correlated with initial diameter (DMPC: $p = 2.2 \times 10^{-5}$; DOPC: $p = 0.05$). (C) Bubble lifetime vs initial diameter. The bubble lifetime is not correlated with initial diameter (DMPC: $r = 0.0214$, $p = 0.7877$; DOPC: $r = 0.1157$, $p = 0.2975$). For all graphs, lines are linear fits, filled symbols are bubbles coated with DMPC in air-saturated buffer, open symbols are bubbles coated with DOPC in air-saturated buffer, green circles are bubbles exposed to 200 kPa 3 cycle ultrasound pulses, black squares are 200 kPa 7 cycles, red triangles are 300 kPa 3 cycles, and plus sign symbols are DMPC bubbles in 200 kPa 3 cycle ultrasound in PFB-saturated buffer.

shrinkage is inactive when the coat density becomes sufficiently high. It is noteworthy, however, that previous studies by us⁷ and others⁹ have found *no correlation* between initial size and transition size, when using coats containing stabilizing PEG-lipids. It unclear how the presence of a small fraction (typically 10 mol %) of PEG-lipid decouples these parameters.

The initial rapid shrinkage rate is somewhat faster for larger bubbles (Figure 5B), and this may partly account for the fact that the overall bubble lifetime is essentially uncorrelated with the initial bubble size (Figure 5C). (The rate of slow phase shrinkage was uncorrelated with initial size. In addition, a significant fraction of bubbles show a very rapid final shrinkage,

like the DOPC bubble in Figure 2; this could also weaken the correlation of lifetime with initial size.)

3.2. Slow Phase Shrinkage and Temperature Dependence. Prior work has shown that the slow phase depends strongly on the species of lipid used in the coat. In particular, bubbles with coats consisting (primarily) of the long chain saturated lipid DSPC exhibited such slow shrinkage that they could be considered “stable” for the duration of the measurement, many hundreds of ultrasound pulses. In contrast, bubbles coated with the unsaturated lipid DOPC showed persistent (slow) shrinkage and typically vanished entirely after 100–200 pulses. These two lipid coats differ in both chemical (bond saturation) and physical (lipid phase) properties. To better understand what factors control bubble stability and slow shrinkage, we prepared bubbles with DMPC or DOPC coats and studied their behavior as a function of temperature. In Figure 6, the mean lifetime of bubbles is plotted vs buffer

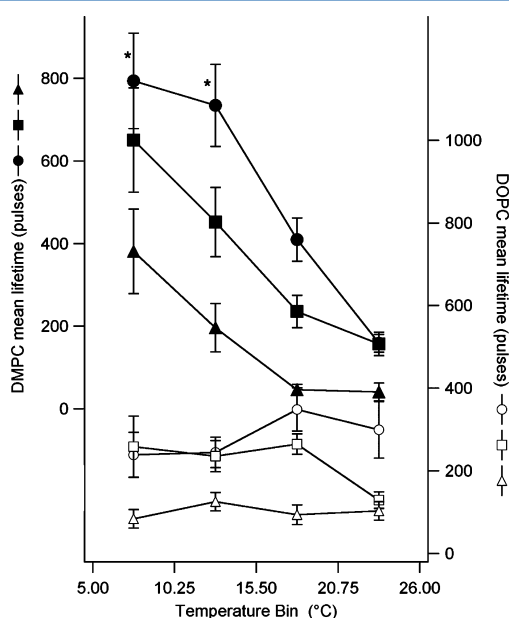


Figure 6. Bubble lifetime vs temperature. Filled symbols are DMPC-coated bubbles, open symbols are DOPC-coated bubbles, circles are bubbles exposed to 200 kPa 3 cycle ultrasound, squares are 200 kPa 7 cycles, and triangles are 300 kPa 3 cycles. The data were binned in temperature; each point is the mean and standard error of the mean (SEM) for each bin. The lowest two DMPC temperature points are statistically different from the highest for every pulse amplitude and duration (200 kPa 3 cycle, $p > 99.9\%$, 200 kPa 7 cycle, $p > 99.5\%$, 300 kPa 3 cycle, $p > 95\%$). The lifetime of bubbles is correlated with temperature for DMPC ($p = 5.05 \times 10^{-5}$) and not correlated for DOPC ($p = 0.28$).

temperature for each coat lipid. Although there is large variability in the data, there is a clear trend toward lower stability for DMPC coats at higher temperatures. The effect is more pronounced with shorter pulses and lower intensities. No such trend was observed for DOPC.

The shorter bubble lifetime at higher temperatures was coincident with more rapid shrinkage in both the rapid and slow phases as well as a smaller transition size (Figure 7). However, the strongest and most significant temperature dependence was found with slow phase shrinkage, with far

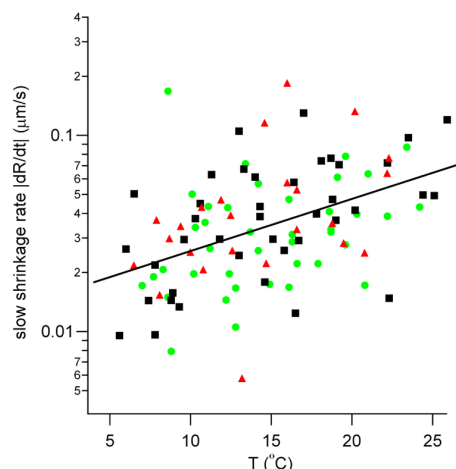


Figure 7. Slow shrinkage rate vs temperature for DMPC bubbles. Green circles are bubbles exposed to 200 kPa 3 cycle ultrasound, black squares are 200 kPa 7 cycles, red triangles are 300 kPa 3 cycles, and the line is a linear fit. The slow shrinkage rate is correlated with temperature ($p = 7.3 \times 10^{-12}$). The slope (when data are plotted against $1/T$) suggests an Arrhenius activation energy of 18.4 kJ, but the small temperature range makes this interpretation tenuous.

less significant changes in both transition size and rapid shrinkage rates.

DMPC monolayers show a fluid to crystalline “main” transition at temperatures below ca. 19 °C; the temperature of the onset of the transition depends on the monolayer density.¹⁸ We suggest that this monolayer transition manifests itself in our bubble stability measurements, with initially condensed or gel phase monolayers giving rise to slower shrinkage and longer bubble lifetimes. The lack of a sharp transition and the breadth of the shrinkage rates and lifetimes at a fixed temperature are to be expected, given the variations in bubble coat densities and radii. It is also noteworthy that the transition in bubble stability becomes less pronounced if longer or stronger ultrasound pulses are used (Figure 6). Interestingly, stronger pulses (300 kPa) also gave a distribution of DMPC-coated bubble fates that more closely resembled that of DOPC-coated bubbles—a much larger fraction of bubbles show visible fragmentation (Figure 3). Clearly, the additional stability provided by the saturated DMPC coat lipid can, at least in part, be overcome by using a longer pulse duration or, even more effectively, stronger pulses (though even with the stronger pulses, there remains a clear temperature dependence, Figure 6.) We speculate that longer or stronger pulses may lead to increased temperature in the vicinity of the bubble, through either viscous heating or stronger adiabatic heating. (Adiabatic heating on compression of the bubble should *always* increase the temperature above the DMPC melting transition, however, as discussed below. Thus, if the diminished temperature response with longer or stronger pulses is due to heating, it must be local heating of the solution, not the oscillatory temperature changes in the bubble gas.)

3.3. Collapse Pressures. The pressure amplitude of the ultrasound pulse is 200–300 kPa, which, in a spherical shell with a radius on the order of micrometers, would give surface pressures of many hundreds of dyn/cm—far above the collapse pressures of lipid monolayers (55 dyn/cm for DMPC¹⁹), regardless of phase state. The fact that the (initial) lipid phase state appears to contribute to bubble stability may seem

remarkable, in consideration of the very high surface pressures reached. In addition, of course, adiabatic heating of the bubble during compression should give rise to highly elevated temperatures (ca. 100 °C, for an initially 3 μm bubble compressed to 100 nm^{7,20}), regardless of the bath temperature.

If lipid monolayer phase plays a role in bubble stability, as our observations imply, it must do so by affecting the initial distribution of lipids on the surface and thus creating spatially varying surface properties that greatly modify the subsequent bubble behavior in the presence of the strong ultrasonic field. We suggest that condensed or crystalline/gel phases, present in DMPC and DSPC monolayers, contain defects between domains that direct the bubble compression in a highly anisotropic manner, for example by leading to “pancaking”. Although such modes of compression are speculative, they offer a mechanism by which lipid coats or shells would remain associated with the bubble throughout the collapse, while avoiding extensive corrugations or invaginations that would more readily micellize or otherwise be shed from the bubble.

4. CONCLUSIONS

We have observed micrometer-scale perfluorobutane bubbles coated with DMPC or DOPC in pulsed ultrasound at temperatures from 4 to 26 °C and found that most bubbles exhibit biphasic shrinkage with an initial rapid phase followed by a much slower phase. The rate of the initially rapid shrinkage was much greater than that allowed by diffusional gas loss, as given by the Epstein–Plesset equation. The bubble size at the transition from one phase to the other was correlated with initial size; this “memory” of the initial size may be dependent on the initial coat density, if the coat remains associated with the bubble during the initial rapid bubble shrinkage.

The lifetime of bubbles coated with DMPC was strongly correlated with temperature, with increased stability at lower temperatures. No such correlation was observed for DOPC bubbles. This suggests that decreased stability in bubbles is due to the fluid phase, rather than the chemical bond saturation, of the lipid coat. This does not rule out a role for the chemical bond unsaturation, of course, and experiments with a very long chain unsaturated lipid, or chemical studies to look for lipid degradation or oxidation, are certainly warranted. The most significant temperature dependence was found with the slow phase shrinkage, which became progressively slower as temperature was reduced.

These experimental results indicate that the resting phase of the lipid coat plays an important role in bubble stability in response to pulsed insonation. Controlling coat phase, and in particular using coats that may show phase changes near body temperature (as has been done with liposomes²¹), is thus an attractive design strategy for responsive bubble-based vehicles for ultrasound-mediated drug delivery.

AUTHOR INFORMATION

Corresponding Author

*E-mail: jthomas@unm.edu.

Notes

The authors declare no competing financial interest.

ACKNOWLEDGMENTS

This work was supported by the “Integrating Nanoscience with Cell Biology and Neuroscience” IGERT program, NSF Grant DGE 0549500.

ABBREVIATIONS

PFB, perfluorobutane; DSPC, distearoylphosphatidylcholine; DOPC, dioleoylphosphatidylcholine; DMPC, dimyristoylphosphatidylcholine; PBS, phosphate buffered saline; PEG, poly(ethylene glycol); PVC, poly(vinyl chloride); EP, Epstein–Plesset.

REFERENCES

- (1) Pitt, W.; Husseini, G.; Staples, B. Ultrasonic drug delivery – a general review. *Expert Opin. Drug Delivery* **2004**, *1*, 37–56.
- (2) Rapoport, N. Phase-shift, stimuli-responsive perfluorocarbon nanodroplets for drug delivery to cancer. *Wiley Interdiscip. Rev. Nanomed. Nanobiotechnol.* **2012**, *4*, 492–510.
- (3) Husseini, G. A.; Rapoport, N. Y.; Christensen, D. A.; Pruitt, J. D.; Pitt, W. G. Kinetics of ultrasonic release of doxorubicin from pluronic P105 micelles. *Colloids Surf., B* **2002**, *24*, 253–264.
- (4) Suslick, K. S.; Price, G. J. Applications of ultrasound to materials chemistry. *Annu. Rev. Mater. Sci.* **1999**, *29*, 295–326.
- (5) Geis, N. A.; Katus, H. A.; Bekereldjian, R. Microbubbles as a vehicle for gene and drug delivery: current clinical implications and future perspectives. *Curr. Pharm. Des.* **2012**, *18*, 2166–2183.
- (6) Duncan, P. B.; Needham, D. Test of the Epstein–Plesset model for gas microparticle dissolution in aqueous media: Effect of surface tension and gas undersaturation in solution. *Langmuir* **2004**, *20*, 2567–2578.
- (7) Cox, D. J.; Thomas, J. L. Ultrasound-induced dissolution of lipid-coated and uncoated gas bubbles. *Langmuir* **2010**, *26*, 14774–14781.
- (8) Cox, D. J.; Thomas, J. L. Rapid shrinkage of lipid-coated bubbles in pulsed ultrasound. *Ultrasound Med. Biol.* **2013**, *39*, 466–474.
- (9) Borden, M. A.; Kruse, D. E.; Caskey, C. F.; Zhao, S. K.; Dayton, P. A.; Ferrara, K. W. Influence of lipid shell physicochemical properties on ultrasound-induced microbubble destruction. *IEEE Trans. Ultrason. Ferroelectr. Freq. Control* **2005**, *52*, 1992–2002.
- (10) Guidi, F.; Vos, H. J.; Mori, R.; de Jong, N.; Tortoli, P. Microbubble Characterization Through Acoustically Induced Deflation. *IEEE Trans. Ultrason. Ferroelectr. Freq. Control* **2010**, *57*, 193–202.
- (11) Jana, A. K.; Agarwal, S.; Chatterjee, S. N. The induction of lipid-peroxidation in liposomal membrane by ultrasound and the role of hydroxyl radicals. *Radiat. Res.* **1990**, *124*, 7–14.
- (12) Rosenthal, I.; Sostaric, J. Z.; Riesz, P. Sonodynamic therapy - a review of the synergistic effects of drugs and ultrasound. *Ultrason. Sonochem.* **2004**, *11*, 349–363.
- (13) Feshitan, J. A.; Chen, C. C.; Kwan, J. J.; Borden, M. A. Microbubble size isolation by differential centrifugation. *J. Colloid Interface Sci.* **2009**, *329*, 316–324.
- (14) Lozano, M. M.; Longo, M. L. Microbubbles coated with disaturated lipids and DSPE-PEG2000: phase behavior, collapse transitions, and permeability. *Langmuir* **2009**, *25*, 3705–3712.
- (15) O'Brien, J.-P.; Ovenden, N.; Stride, E. Accounting for the stability of microbubbles to multi-pulse excitation using a lipid-shedding model. *J. Acoust. Soc. Am.* **2011**, *130*, EL180–EL185.
- (16) Epstein, P. S.; Plesset, M. S. On the stability of gas bubbles in liquid-gas solutions. *J. Chem. Phys.* **1950**, *18*, 1505–1509.
- (17) Thomas, D. H.; Butler, M.; Anderson, T.; Emmer, M.; Vos, H.; Borden, M.; Stride, E.; de Jong, N.; Sboros, V. The “quasi-stable” lipid shelled microbubble in response to consecutive ultrasound pulses. *Appl. Phys. Lett.* **2012**, *101*.
- (18) Albrecht, O.; Gruler, H.; Sackmann, E. Polymorphism of phospholipid monolayers. *J. Phys.* **1978**, *39*, 301–313.
- (19) Borden, M. A.; Longo, M. L. Dissolution behavior of lipid monolayer-coated, air-filled microbubbles: Effect of lipid hydrophobic chain length. *Langmuir* **2002**, *18*, 9225–9233.
- (20) Morgan, K. E.; Allen, J. S.; Dayton, P. A.; Chomas, J. E.; Klivanov, A. L.; Ferrara, K. W. Experimental and theoretical evaluation of microbubble behavior: Effect of transmitted phase and bubble size. *IEEE Trans. Ultrason. Ferroelectr. Freq. Control* **2000**, *47*, 1494–1509.

(21) Needham, D.; Dewhirst, M. W. The development and testing of a new temperature-sensitive drug delivery system for the treatment of solid tumors. *Adv. Drug Delivery Rev.* **2001**, *53*, 285–305.